27/28th International Conference
ENGINEERING MECHANICS 2022
Milovy, Czech Republic, May 9 –12, 2022
Paper **#50,** pp. 165–168, doi: 10.21495/51-2-165

CFD ANALYSIS OF FREE SURFACE VORTEX SHAPE IN AN UNBAFFLED STIRRED TANK

Illík J. [*], **Štigler J.** [**]

Abstract: *Stirred tanks are widely used in the chemical industry. There is plentiful research on the fluid flow characteristics within such vessels, mainly aimed at mixing optimization. This work focuses on the shape of the free surface formed into a vortex due to centrifugal effects. The two-phase simulation is performed with the Volume of Fluid (VOF) method and solely uses the Reynolds Stress Model (RSM) turbulence model. The accuracy of two RSM submodels is evaluated. The computational grid is stationary, and the rotation of the impeller is simulated using the Multiple Reference Frame (MRF) method. The calculation process is compared to the previous work, where also $k-\varepsilon$ turbulence model had to be used before switching to the RSM model. Further evaluation of the vortex shape is conducted on geometry without the impeller. The method of fitting the free surface with a curve based on the Cauchy probability density function is presented. The tangential velocity profile can be derived from the fitted curve – mainly for the deep vortex since the accuracy is limited.*

Keywords: Stirred tank, Multiphase flow, Reynolds Stress Model, Vortex shape, Cauchy distribution.

1. Introduction

Fluid flow in stirred tanks has been studied experimentally (Busciglio et al., 2013) and using numerical simulations by many researchers (Li & Xu, 2017). Simpler two-equation turbulence models, such as $k-\varepsilon$ and $k-\omega$ are being compared (Haque et al., 2011) with more complex models. The Reynolds Stress Model (RSM) model used in this work can accurately model the high swirling flow. More demanding approaches like Large Eddy Simulation (LES) or Direct Numerical Simulation (DNS) can give even more precise results (Tamburini et al., 2021) but at a higher computational cost.

2. Methods

The Reynolds-averaged Navier–Stokes (RANS) equation are time-averaged equations

$$\frac{\partial}{\partial t}\left(\rho\,\overline{v_i}\right)+\frac{\partial}{\partial x_j}\left(\rho\,\overline{v_i}\,\overline{v_j}\right)=-\frac{\partial \overline{p}}{\partial x_i}+\frac{\partial}{\partial x_j}\left[\mu\left(\frac{\partial \overline{v_i}}{\partial x_j}+\frac{\partial \overline{v_j}}{\partial x_i}-\frac{2}{3}\delta_{ij}\frac{\partial \overline{v_k}}{\partial x_k}\right)\right]+\frac{\partial}{\partial x_j}\left(-\rho\overline{v_i'v_j'}\right), \qquad (1)$$

where the last term, Reynolds stresses $R_{ij}=-\rho\overline{v_i'v_j'}=\tau_{t_{ij}}$ (viscous or apparent stress), is the core of RANS turbulence modelling. While the two-equation models use the Boussinesq hypothesis (isotropic turbulence) and therefore have 1 transport equation for the turbulent kinetic energy, the RSM model works with 6 transport equations. Both have 1 more transport equation for the rate of dissipation of turbulent kinetic energy. RSM model can model high swirling flow, where the turbulence is not isotropic, but it is more computationally demanding and more prone to convergence difficulties.

[*] Ing. Jakub Illík: Viktor Kaplan Department of Fluid Engineering, Energy Institute, Brno University of Technology, Technická 2896/2; 616 69, Brno; CZ, 183640@vutbr.cz

[**] doc. Ing. Jaroslav Štigler, Ph.D.: Viktor Kaplan Department of Fluid Engineering, Energy Institute, Brno University of Technology, Technická 2896/2; 616 69, Brno; CZ, stigler@fme.vutbr.cz

2.1. Computational model

The computational grid is created in the ANSYS® Meshing™ software. The mesh in this work is referred to as Mesh 2 (see Tab. 2). It is more refined than the Mesh 1 in the previous work (Illík, 2020) in order to conduct the simulation directly using the RSM model. The 3D transient simulation was performed using the ANSYS® Fluent® software with solver settings listed in Tab. 1. The simulation setup is inspired by the work of Vlček et al. (2013). The tank is cylindrical ($H = 180$ mm, $D = 150$ mm) and the impeller has two 13 mm blades attached to the rod ($d = 10$ mm). The MRF zone must be closely adjacent to the rotating part, in this case, the zone is a cylinder with 44 mm diameter and 19 mm height. Simulated phases are water and air. The tank is filled with water up to a height of 126 mm. The horizontal reference plane for CFD analysis is 80 mm above the bottom (Fig. 3). Operating conditions: gravity and atmospheric pressure. Free surface profiles are presented from the mentioned previous work, where Mesh 1 was modified to Mesh 1d (geometry without the impeller, similar grid size), and the diffusion of the created vortex was observed.

Tab. 1: Solver settings

Impeller	blade 13 mm, $n = 600\ \mathrm{min}^{-1}$
Methods and models	VOF, MRF, RSM-SSG, Scalable WF
Discretization	LSCB, PRESTO!, HRIC, 2^{nd} Upwind, t 2^{nd} Implicit

2.2. Vortex shape analysis

The probability density function of the Cauchy distribution can be written as (Feller, 1957):

$$f(x) = \frac{1}{\pi\gamma}\left[\frac{\gamma^2}{(x-x_0)^2+\gamma^2}\right]. \tag{2}$$

In physics, this distribution can be used for analyzing the roentgen spectrum, where γ is the scale parameter, which specifies the half-width at half-maximum (HWHM), and x_0 is the location parameter that describes the position of the peak of the distribution. Term $\frac{1}{\pi\gamma}$ represents the amplitude. The idea to use a curve based on this distribution for fitting the shape of the free surface vortex comes from these three parameters, which can be easily adjusted. Gauss distribution is also considered (see Fig. 1), but the function converges too fast to zero value (of probability or, in this case, vortex depth). The fit is done by using a script (Wells, 2020) based on Cauchy (also Lorentzian) distribution. The equation from this script can be rewritten for fitting the free surface described in cylindrical coordinates:

$$h(r) = \frac{c_1}{(r-c_2)^2+c_3} + h_0, \tag{3}$$

where coefficients c_1 [mm^3], c_2 [mm] and c_3 [mm^2] shapes the final curve (height, centering, width). The depth of the vortex h is a function of the radius r. In the Cauchy distribution, there is no offset from zero value, but for adjusting the vertical position of the fitted curve, coefficient h_0 is used. The tangential velocity is derived from Euler's equation and by derivation of the fitted Cauchy curve from Eq. (3) (Illík, 2020):

$$v_t = \sqrt{g\,r\,\frac{\mathrm{d}h(r)}{\mathrm{d}r}} = \sqrt{2g\,c_1\,\frac{r(r-c_2)}{\left[(r-c_2)^2+c_3\right]^2}}. \tag{4}$$

Fig. 3 shows similar results for tangential velocity obtained from the Cauchy fit (only for deep vortex, early stage of diffusion) and prediction by the Burnham-Hallock vortex model (Burnham & Hallock, 1982):

$$v_t = \frac{\Gamma_0}{2\pi r}\frac{r^2}{r^2+r_c^2}, \tag{5}$$

where Γ_0 is the initial circulation and r_c is the radius of the vortex core. Both are extracted from CFD data for plotting the models' predictions in Fig 3. First term in Eq. (5) is equal to the Rankine vortex model for $r > r_c$ and the second term is similar to the form of Eq. (4) for axisymmetric (centered) vortex ($c_2 = 0$).

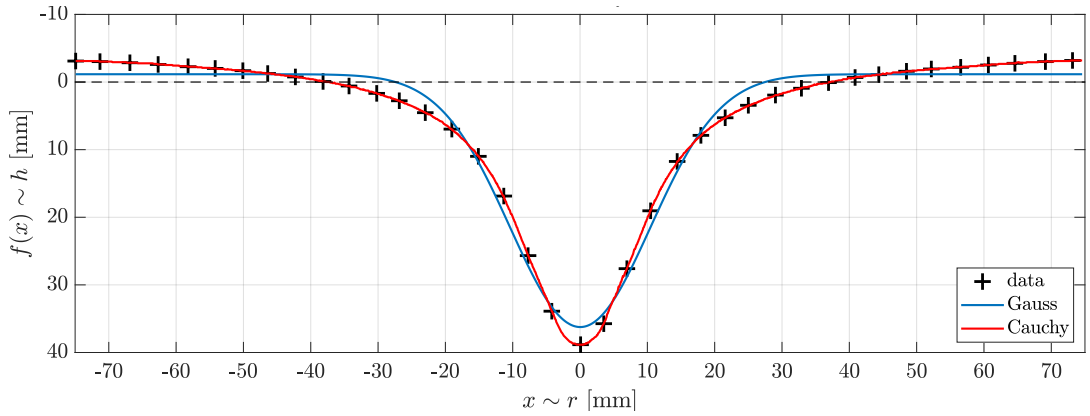

Fig. 1: Free surface from the simulation fitted with Cauchy and Gauss curves. The depth h is negative near the tank walls – this effect would be minimized inside a larger tank, depth is calculated respective to the dashed line representing the calm free surface. Case of vortex diffusion ($t = 1$ s). Mesh 1d.

3. Results and discussion

Both RSM submodels for pressure strain term were applied. The linear, Launder-Reece-Rodi (LRR) was active for the first 15 s of the calculation. Then the quadratic submodel, Speziale-Sarkar-Gatski (SSG) was switched on for another 15 s. Copy of the initial LRR calculation was kept running until the final 30 s for comparison with the SSG. The results for 30 s are shown in Fig. 2. The SSG gives a better defined water-air interface. Also, less amount of air is trapped below the impeller in the SSG simulation.

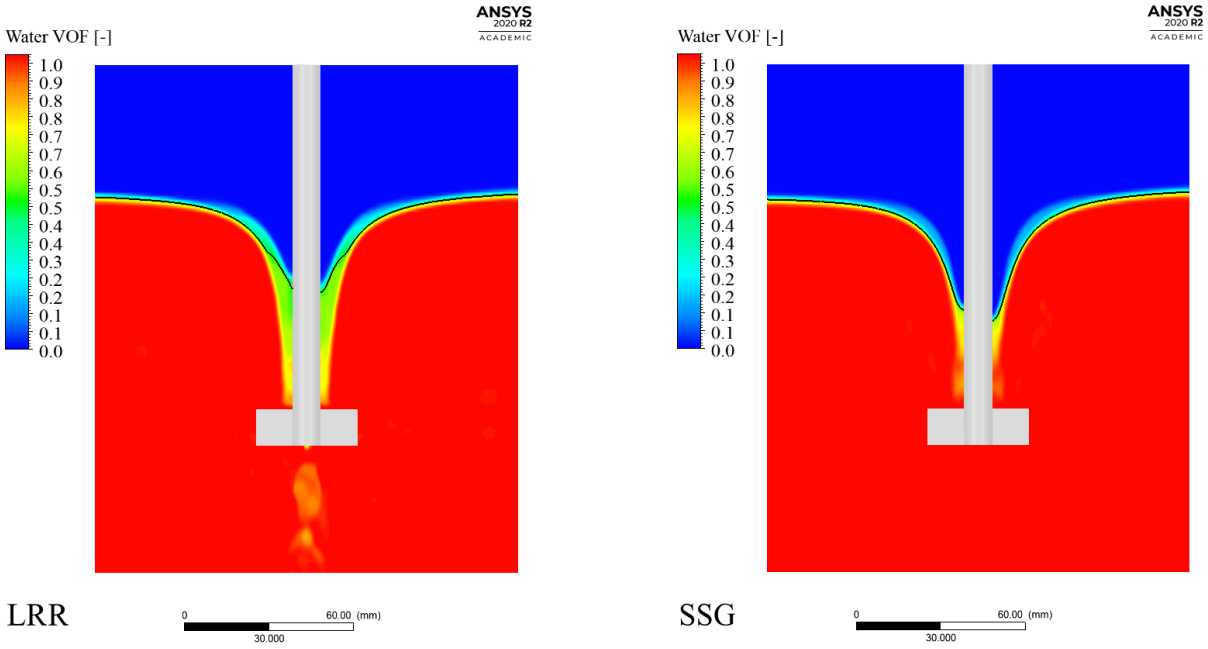

Fig. 2: Comparison of the two RSM submodels: LRR (left), SSG (right). The black line represents the approximate free surface (VOF $= 0.5$). Case of stirring ($t = 30$ s). Mesh 2.

The original purpose of these simulations was the creation of a precise shape of a deep enough vortex, so the diffusion of this vortex could be observed. In other studies, a different impeller with multiple blades is used (Rushton turbine). The influence of various RPM, blade size, or impeller distance from the tank bottom is presented in (Li & Xu, 2017). The free surface from simulation and experimental results (Busciglio et al., 2013) are often compared with the widely used Nagata model (Nagata, 1975).

Tab. 2: Calculation comparison

	elements	type	formulation	turb. model	time	max. step	iterations	residuals
Mesh 1	511 775	hexa	steady, transient	$k-\varepsilon$, RSM	20 s	0.005 s	60 000	10^{-5}
Mesh 2	2 806 534	hexa	transient	RSM	30 s	0.002 s	350 000	10^{-4}

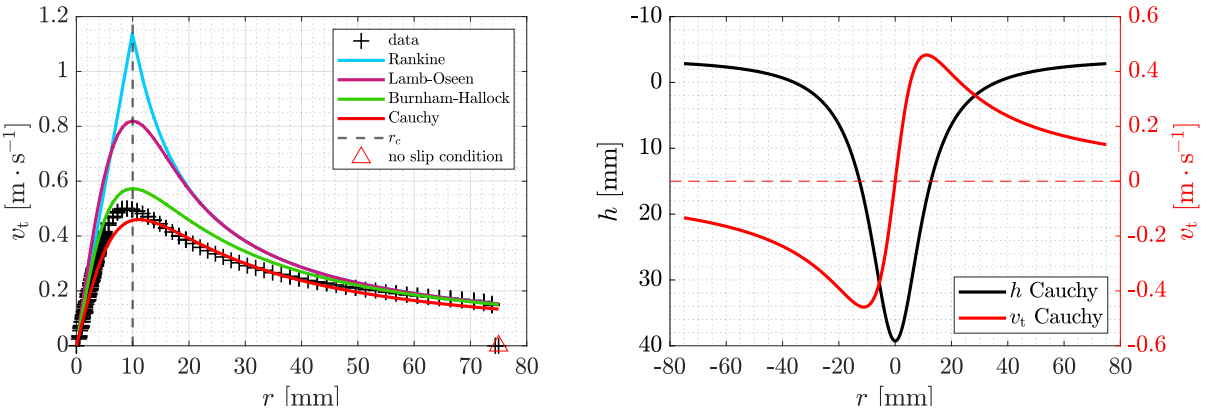

Fig. 3: Tangential velocity – vortex models' predictions and simulation data. Plotted values are for the reference plane, Cauchy prediction is for the free surface (left). Vortex shape with complete velocity profile at free surface [red] extracted from Cauchy fit [black] (right). Case of vortex diffusion ($t = 1$ s). Mesh 1d.

4. Conclusions

The transient simulation of unbaffled stirred cylindrical tank was performed using the RSM model, and two submodels (LRR, SSG) were compared. The calculation was set directly to RSM without using the $k-\varepsilon$ model first. The simulation was able to proceed, but a lower timestep had to be used. However, the final vortex shape is not so dependent on the iteration process as long as the last turbulence model used is RSM-SSG, which provides the best result of the tested models ($k-\varepsilon$ Standard, RSM-LRR, RSM-SSG). Free surface (vortex diffusion) can be fitted with a curve obtained from the Cauchy distribution. The tangential velocity profile can be derived from this curve, but the estimates are applicable only for a deep vortex shape.

References

Burnham, D. C. & Hallock, J. N. (1982), Chicago Monostatic Acoustic Vortex Sensing System. In: *Vol. IV: Wake Vortex Decay*. Cambridge, MA, National Transportation Systems Center (U.S.), DOT/FAA/RD-79-103, IV, DOT-TSC-FAA-79-18, IV.

Busciglio, A., Caputo, G. & Scargiali, F. (2013), Free-surface shape in unbaffled stirred vessels: Experimental study via digital image analysis. *Chemical Engineering Science*, Vol. 104, pp. 868-880.

Feller, W. (1957), *An introduction to probability theory and its applications*, John Wiley & Sons, New York.

Haque, J. N., Mahmud T., Roberts, K. J., Liang, J. K., White, G., Wilkinson, D. & Rhodes, D. (2011), Free-surface turbulent flow induced by a Rushton turbine in an unbaffled dish-bottom stirred tank reactor: LDV measurements and CFD simulations. *The Canadian Journal of Chemical Engineering*, Vol. 89, No. 4, pp. 745-753.

Illík, J. (2020), Fluid flow analysis in the open cylindrical container with the free surface vortex. Master's thesis, Brno University of Technology, Faculty of Mechanical Engineering, Brno, [Czech language].

Li, L. & Xu, B. (2017), Numerical simulation of hydrodynamics in an uncovered unbaffled stirred tank. *Chemical Papers*, Vol. 71, No. 10, pp. 1863-1875.

Nagata, S. (1975), *Mixing Principles and Applications*, John Wiley & Sons, New York.

Tamburini, A., Brucato, A., Ciofalo, M., Gagliano, G., Micale, G. & Scargiali, F. (2021), CFD simulations of early- to fully-turbulent conditions in unbaffled and baffled vessels stirred by a Rushton turbine. *Chemical Engineering Research and Design*, Vol. 171, pp. 36-47.

Vlček, P., Skočilas, J. & Jirout, T. (2013), CFD simulation of a stirred dished bottom vessel. *Acta Polytechnica*, Vol. 53, No. 6, pp. 906-912.

Wells, J. (2020), lorentzfit(x,y,varargin). *MATLAB Central File Exchange*, 2020, [/33775-lorentzfit-x-y-varargin].